

## Article

# Mitogenome Assembly Reveals Gene Migration and RNA Editing Events in Plateau Hongliu (*Myricaria elegans* Royle.)

Xue Li <sup>1,†</sup>, Hao Wu <sup>1,†</sup>, Xingyao Hu <sup>1</sup>, Yunhua Wu <sup>2</sup>, Feng Nie <sup>2</sup>, Tao Su <sup>1,\*</sup>, Mei Han <sup>1,\*</sup> and Fuliang Cao <sup>3</sup>

<sup>1</sup> Co-Innovation Center for Sustainable Forestry in Southern China, State Key Laboratory of Tree Genetics and Breeding, College of Life Sciences, Nanjing Forestry University, Nanjing 210037, China

<sup>2</sup> Forestry Survey and Planning Institute of Tibet, Lhasa 850032, China

<sup>3</sup> College of Forest, Nanjing Forestry University, Nanjing 210037, China

\* Correspondence: sutao@njfu.edu.cn (T.S.); sthanmei@njfu.edu.cn (M.H.); Tel.: +86-1589-598-3381 (T.S.)

† These authors contributed equally to this work.

**Abstract:** The Plateau Hongliu (*Myricaria elegans* Royle.) is a woody shrub halophyte that thrives in arid areas of western Tibet, in the Himalayan Mountains. It is acclaimed as superior in saline stress acclimation and as a critical pharmaceutical resource of the Tibetan traditional herb. Nevertheless, the mitogenome in the genus *Myricaria* remains unknown. Here, using the Illumina and PacBio sequencing assays, the first complete mitogenome of the *M. elegans* revealed a multi-branched skeleton with a total length of 416,354 bp and GC content of 44.33%, comprising two circular molecules (M1 and 2). The complete mitogenome annotates 31 unique protein-encoding genes (PEGs), fifteen tRNAs, and three rRNA genes. The UAA exhibits the most prominent codon usage preference as a termination, followed by UUA codons for leucine. The mitogenome contains 99 simple sequence repeats and 353 pairs of dispersed repeats, displaying the most frequent in palindromic repeats. Gene transfer analyses identified 8438 bp of 18 homologous fragments from the plastome, accounting for 2.03% of the total length. Using the PREP suite, 350 C-U RNA editing sites were predicted, of which *nad4* and *ccmB* were on the top frequency. Syntenic and phylogenetic analyses suggested weakly conserved patterns of *M. elegans* in Caryophyllales owing to the genome rearrangement. In summary, the deciphered unique features and complexities of the mitogenome in *M. elegans* provide novel insights into understanding the evolution and biological conservation underlying climate resilience in halophytes.



**Citation:** Li, X.; Wu, H.; Hu, X.; Wu, Y.; Nie, F.; Su, T.; Han, M.; Cao, F. Mitogenome Assembly Reveals Gene Migration and RNA Editing Events in Plateau Hongliu (*Myricaria elegans* Royle.). *Forests* **2024**, *15*, 835.

<https://doi.org/10.3390/f15050835>

Received: 13 April 2024

Revised: 2 May 2024

Accepted: 8 May 2024

Published: 10 May 2024



**Copyright:** © 2024 by the authors. Licensee MDPI, Basel, Switzerland. This article is an open access article distributed under the terms and conditions of the Creative Commons Attribution (CC BY) license (<https://creativecommons.org/licenses/by/4.0/>).

**Keywords:** *Myricaria elegans*; halophyte; mitogenome; RNA editing; genome recombination

## 1. Introduction

The *Myricaria elegans* Royle. belongs to the family Tamaricaceae, namely Plateau Hongliu (Tibetan: Hongbu), due to striking reddish-brown branchlets in barks, which produce lateral inflorescences resembling spikes adorned with pink/purplish-red flowers [1]. It is a xylophyta that grows at high altitudes (3500–4800 m) and is predominantly in the China Tibet (Ngari Prefecture) and arid areas of western Himalaya (e.g., Ladakh and Kashmir) [2]. They thrive in extreme climates and saline-alkaline lands, prompting them to be the origin of the genus *Myricaria* to study genetic evolution and ecological adaptation to harsh environments, particularly in high-altitude mountains [3]. During the ancient and current ages, *M. elegans* was used by indigenous people in western Tibet as an ethnological herb to alleviate injuries, including bruises, wounds, and burns [4]. The phytochemical assay determined the enrichment of pentacyclic triterpenes, phenols, flavonoids, and other bioactive constituents in fractions of dried aerial parts, implicating conspicuous pharmacological potentials of *M. elegans* in anti-nociception and anti-inflammation [5]. Despite the ecological and pharmaceutical importance, the comprehensive genetic and molecular basis, including the mitogenome and nuclear genome, have not been attempted in the *M. elegans*.

Plant cells integrate two energy-generating compartments, mitochondria and plastids, originating from ancestors of symbiotic bodies in prokaryotes [6]. As semi-autonomous and highly dynamic organelles, the mitochondria house their DNA, RNA, and ribosomes, possessing independent replication, transcription, and translation systems that can produce a few mitochondrial proteins [7]. Through oxidative phosphorylation, mitochondria provide essential energy (ATP) for driving cellular functions, and they also play crucial roles in photorespiration, homeostasis, stress responses, and other diverse metabolic regulation [8]. Unlike nuclear genes, mitochondrial DNA usually has a matrilineal inheritance mode rather than passing on through both parents in most terrestrial plants, suggesting host population fitness and organellar genome stability [9]. The mitochondria's unique cellular structure and biochemical properties make them significant in diverse functions [10].

The plant mitogenome exhibits a more structural complexity and significant length variation than animals due to the abundance of repetitive sequences [11]. The plant mitogenome was thought to hold a conventional, single-circular chromosomal structure based on the widely-held view of the broad science community. However, many reports suggest this is an inaccurate and outdated concept [12]. Undergoing genome replication, frequent homologous recombination, gene loss or transfer to the plastome or nuclear genome, and the conformation and size of plant mitogenome between different lineages are variable [13,14]. Most of the plant mitogenome assembled displayed as a single circular map reported in some plants, including *Arabidopsis thaliana* (L.) Heynh., *Suaeda glauca* (Bunge) Bunge., zucchini, and some crops [15–20]. A few cases exist where the mitogenomes are linear DNA molecules or linear-circular combinations, as evidenced in rice and spearmint [21,22]. Early renaturation DNA kinetics and polymorphism analysis estimated that the size diversity of mitogenomes varied tremendously in different plants or even among closely related species, ranging from 200 kb to 3 Mb [23]. However, the complete sequences can be expanded from the minimal size of 66 kb (*Viscum scurruloideum* Barlow.) to a large size of 11.3 Mb (*Silene conica* L.) using the advanced sequencing technique [24,25]. The mitogenome size is not linearly correlated with the number of encoded genes but depends much on mutation rates that favor reduced/increased mitogenome size and complexity [26].

The mitogenome contains many RNA editing sites and nucleotide sequence polymorphisms (repeats) associated with the variability and mitogenome recombination [27]. RNA editing events typically maintain the conserved amino acids in essential proteins and generate new start or stop codons, affecting gene translation processes and altering the proteins' length and function [28,29]. The horizontal transfer of homologous segments between different genomes plays a crucial role in the evolution of the plant mitogenome. Exploring variations and recombination based on the complete mitogenome offers advantages in phylogenetic reconstruction, classification, and environment adaptation [30]. To achieve this, we employed the Illumina integrated with PacBio sequencing technology to generate the first high-quality mitogenome of the *M. elegans* with available accession IDs (OP429117 and OP429118) in GenBank. The de novo mitogenome assembly, annotation, and extensive survey of the genetic backgrounds provide novel insight into the functional role in DNA/RNA changes, plant evolution, and germplasm conservation in the genus *Myricaria*.

## 2. Materials and Methods

### 2.1. Plant Materials, DNA Extraction, and Sequencing

The fresh leaves of the *M. elegans* were collected from the Jiamu Hongliu Wetland Park, Sengezangbu Town, Gar County (Nigari, Tibet), located at coordinates 32°27'13" N, 80°9'56" E, with an altitude of 4342 m. The voucher specimen (ID: ST20210502002) was deposited in the herbarium of the Nanjing Forestry University, Nanjing, Jiangsu Province. High-quality genomic DNA was isolated using the CTAB method [31]. The quality and concentration of DNA samples were evaluated with agarose gel electrophoresis and a Nanodrop 2000C UV/Vis Spectrophotometer (Thermo, Waltham, MA, USA). The qualified DNA samples were sent to Wuhan Benagen Technology Co., Ltd. (Wuhan, China, <http://en.benagen.com/>,

accessed on 12 May 2022) using the hybrid platforms of the Illumina, NovaSeq 6000 (Illumina, San Diego, CA, USA), and PacBio RS SMRT (Pacific Biosciences, Menlo Park, CA, USA) for library construction and sequencing.

## 2.2. Mitogenome Assembly and Gene Annotation

The mitogenome was assembled using a hybrid assembly strategy using short-read Illumina and long-read PacBio sequencing data. The sequence assembly of Illumina short-reads was performed using the GetOrganelle software (v1.7.7.1 5 January 2023) with default parameters to obtain a graphical plant mitogenome [32]. The assembled mitogenome was visualized using the Bandage software (v0.9.0 20 July 2015) to remove single extended fragments from the plastome and nuclear genome [33]. The PacBio long-read data were then compared to the graphical mitogenome fragments using BWA software (v0.7.1 7 November 2017) to guarantee the accuracy of the assembled mitogenome [34]. The resulting PacBio sequencing data were used to resolve repetitive sequence regions and ensure the consistency between the short-reads and long-reads in the final graphical mitogenome of *M. elegans*. The *A. thaliana* was selected as the reference genome for annotating the protein-encoding genes (PEGs) that were conducted by using the Geseq software (v2.03 18 December 2020) [35]. The tRNA genes of the mitogenome were annotated using tRNAscan-SE software (v2.0.12 20 September 2021) [36]. The metagenomics rRNAs were annotated using the HS-BLASTN software (v2.15.0 18 September 2015) [37]. Apollo software package (v2.7.0 2023.01.04) was used to correct the annotation errors in each mitogenome (<https://github.com/GMOD/Apollo/releases/tag/2.7.0>, accessed on 12 April 2024).

## 2.3. Analysis of Codon Usage Bias and Sequence Repeats

RSCU measures the preference of a specific codon used among synonymous codons, encoding the same amino acid with more significant values. The PEGs of the mitogenome were extracted using the PhyloSuite software (v1.2.3 18 February 2023) [38]. The Mega X software (v10.2.5 March 2021) was used to analyze mitochondrial PEGs for the codon usage preference and RSCU values calculation [39]. The software of the MISA (v2.1 25 August 2020), TRF (v4.09 20 October 2022), and REPuter (v1.0 6 July 2016) were used to identify the repetitive sequences, including the microsatellite sequence repeats (SSRs), tandem repeats, and scattered repeats [34,40,41]. The results were visualized using the RCircos package (v1.2.2 19 December 2021) [42]. The GetOrganelle software (v1.7.7.0 5 January 2023) generated different conformations for the repeat region in a graphical mitogenome [32]. A comparison of the long-read sequence and the repetitive sequences was performed using BWA software to determine whether the repeat region has long-reads spanning and deduce the primary structure in the mitogenome [34].

## 2.4. Sequence Migration Analysis

To identify the MTPTs, the plastome assembly was conducted using the GetOrganelle software with default parameters [32]. The plastidic genes were annotated using the CPGAVAS2 online program (v2 31 March 2019) [43]. Homologous fragments (MTPTs) between the plastome and mitogenome were analyzed using the HS-BLASTN software with an e-value cutoff of  $1 \times 10^{-5}$  [37]. The gene transfer results were visualized using the RCircos package in the TBtools software (v2.070 3 August 2020) [44]. The long-reads were mapped by blasting the reference sequences (mitochondrial and flanking sequences) to confirm the MTPTs using the BWA software [34]. The Tablet software (v1.21 8 February 2021) was used to visualize the sequence migration and homologous mapping [45].

## 2.5. Prediction RNA Editing Sites and Experimental Validation

The RNA editing events in the mitogenome were predicted based on the PREP suite online program (v1.0 25 August 2009) [46]. The SnapGene ([www.snapgene.com](http://www.snapgene.com), accessed on 1 January 2024) (v7.2.0 19 September 2024) was used to design primers for experimental

evaluation of the RNA editing sites, as detailed in Table S13. DNA/RNA was extracted using the DNA/RNAprep Pure Plant Plus Kit (TianGen, Beijing, China). The quality of DNA/RNA samples was evaluated by a UV/Vis spectrophotometer, Nanodrop 2000C (Thermo, Waltham, MA, USA). The cDNA was reverse transcribed from the extracted RNA using the HiScript III 1st Strand cDNA Synthesis Kit (Yugong Biotech, Lianyungang, China). The PCR amplification mix was loaded into the Mastercycler<sup>®</sup> nexus—PCR thermal cycler (Eppendorf, Hamburg, Germany) and performed as an instruction described (2  $\mu$ L DNA/cDNA, 2  $\mu$ L primers, and 25  $\mu$ L 2  $\times$  Taq Master Mix) using the program (pre-denaturation 95  $^{\circ}$ C, 3 min, denaturation 95  $^{\circ}$ C, 15 s, annealing 54  $^{\circ}$ C, 12 s, extension 72  $^{\circ}$ C, 15 s, 35 cycles, and the final extension 72  $^{\circ}$ C, 5 min). The PCR-amplified products were subjected to 1.5% agarose gel electrophoresis, and those with the correct bands were collected to sequence (Sangon, Shanghai, China). The blasted Sanger sequencing results are provided in the Supplementary File S2.

### 2.6. Synteny and Phylogenetic Analysis

The multiple complete mitogenomes were collected and compared to investigate the collinearity relationship between the genetically related species using the HS-BLASTN software [37]. The homologous sequences over 500 bp were collected as conserved colinear blocks to generate the multiple synteny plots using the MCscanX package (<https://github.com/wyp1125/MCScanX>, accessed on 12 April 2024) (vX 11 November 2013) [47]. For the evolutionary analyses, the MAFFT software (v7.525 March 2024) was used for multiple mitogenome sequence alignments [48]. The MrBayes software (v 3.2 1 August 2001) was used as a program for the Bayesian estimation of phylogeny [49]. The PhyloSuite software was used to extract the homologous PEGs within complete mitogenomes between various selected species, and the resulting unrooted phylogenetic tree was visualized using the iTOL software (v6.9 2 July 2021) [38,50].

## 3. Results

### 3.1. Mitogenome Assembly, Structure, and Annotation of the *M. elegans*

In this study, the mitogenome assembly of the *M. elegans* was conducted by using the Illumina and PacBio single molecule real-time (SMRT) sequencing platforms to generate 20.00 Gb (average length: 150 bp) short-reads and 14.996 Gb (average length: 15,670 bp) long-reads data, achieving 1642 raw reads (25.062 Mb), 21 contigs, and depth of 56  $\times$  coverage (Table S1). Due to the frequent rearrangements and recombination in mitogenomes, their structure may not be a simple circular ring, and other substructures may exist [11]. Using the Bandage software, a multi-branched configuration of the draft mitogenome was visualized, including 21 nodes linked to form overlapping zones, repeat regions (red color), and transferred homologous sequences in the green-colored plastome (Figure 1a). After removing duplicated regions combined with PacBio sequencing data, the major assembled mitogenome of the *M. elegans* showed a conformation holding a total length of 416,354 bp (44.33% GC) (Figure 1a and Table S2). The mitogenome was separated into two circular contigs/molecules (M1 and 2), comprising 221,573 bp (M1, GC = 44.32%) and 194,781 bp (M2, GC = 44.33%), respectively. In the sequencing data, the PacBio-based assembly map revealed a total of six pairs of sequence repeats (e.g., nodes 14-22-7, 28, 44, 45, 47, and 48), ranging from 100 to 19,671 bp in length that may mediate the mitogenome recombination (Tables 1 and S2).

**Table 1.** Path analyses in various repetitive regions (nodes) based on PacBio sequencing.

Molecule	Type	Path
M1	circular	10-7-22-14-1-46-13-45-5-47-4-28
M2	circular	11-44-48-6-48-12-45-3-7-22-14-9-47-2-44-8-28

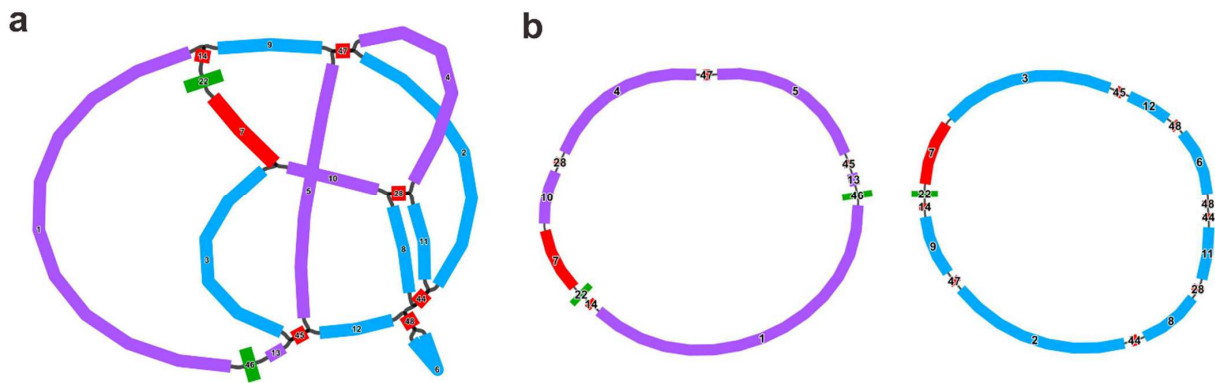


**Figure 1.** Schematic mitogenome structure of the recombination mediated by repetitive sequences in *M. elegans*. (a) Multi-branched conformation of the mitogenome. (b) Two circular molecules (M1, purple, and M2, blue) assembled based on the Illumina and PacBio sequencing data. Repeat regions and transferred homologous sequences were labeled red and green, respectively.

The annotation revealed 31 unique protein-encoding genes (PEGs) in the mitogenome of *M. elegans* (Figure 2 and Table 2). Among them, 24 PEGs were classified into the mitochondrial structural genes, and 7 PEGs were non-core genes, including a single large subunit of the ribosomal gene (*rpl5*) and 6 small subunit ribosomal genes (*rps3*, 4, 7, 10, 12, and 13). The mitochondrial structure genes comprised five ATP synthase (*atp1*, 4, 6, 8, and 9), nine NADH dehydrogenase (*nad1*, 2, 3, 4, 4L, 5, 6, 7, and 9), four ubiquinol cytochrome c biosynthesis (*ccmB*, C, Fc, and Fn), three cytochrome c oxidase (*cox1*, 2, and 3), one membrane transport (*mttB*), one maturase (*matR*), and one cytochrome b (*cob*). Additionally, fifteen tRNA genes (e.g., *trnC-GCA*, *trnN-GUU*, and *trnM-CAU*) and three duplicated rRNA genes (*rrn5*, *rrn18*, and *rrn26*) were identified as non-PEGs anchored in either M1 or M2.

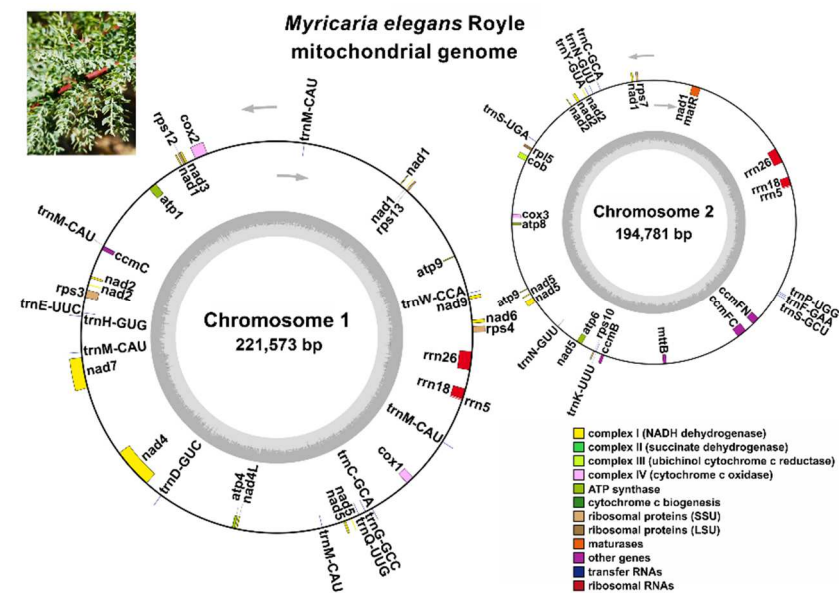


**Figure 2.** The mitogenome map and gene annotations of the *M. elegans*. Annotated genes showed locations inside/outside the circle and transcribed clockwise/counterclockwise labeled by the gray arrow. The GC content was depicted in the inner circle, which was colored in a dark gray.

**Table 2.** The list of the annotated genes in the mitogenome of the *M. elegans*.

Gene Group	Gene Name
ATP synthase	<i>atp1, atp4, atp6, atp8, atp9</i> ( $\times 2^2$ )
NADH dehydrogenase	<i>nad1, nad2, nad3, nad4, nad4L, nad5, nad6, nad7, nad9</i>
Cyt <sup>1</sup> b reductase	<i>cob</i>
Ubiquinol Cyt c biosynthesis	<i>ccmB, ccmC, ccmFC, ccmFN</i>
Cyt c oxidase	<i>cox1, cox2, cox3</i>
Maturase	<i>matR</i>
Membrane transport protein	<i>mttB</i>
Ribosome large subunit	<i>rpl5</i>
Ribosome small subunit	<i>rps3, rps4, rps7, rps10, rps12, rps13,</i>
Ribosome RNA	<i>rrn5</i> ( $\times 2$ ), <i>rrn18</i> ( $\times 2$ ), <i>rrn26</i> ( $\times 2$ )
Transfer RNA	<i>trnC-GCA</i> ( $\times 2$ ), <i>trnD-GUC</i> , <i>trnE-UUC</i> , <i>trnF-GAA</i> , <i>trnH-GCC</i> , <i>trnH-GUG</i> , <i>trnK-UUU</i> , <i>trnM-CAU</i> ( $\times 5$ ), <i>trnN-GUU</i> ( $\times 2$ ), <i>trnP-UGG</i> , <i>trnQ-UUG</i> , <i>trnS-GCU</i> , <i>trnS-UGA</i> , <i>trnW-CCA</i> , <i>trnY-GUA</i>

<sup>1</sup> Cyt, cytochrome. <sup>2</sup> The number represents the gene's copies.

### 3.2. Codon Usage and the Preference of the PEGs

Using the PhyloSuite and Mega, the codon usage preference on 31 PEGs was isolated, and relative synonymous codon usage (RSCU) values were calculated (Figure 3 and Table S3). Based on the criteria, values of RSCU > 1 were considered to be significant for amino acids. Except for the start codon, methionine (Met, AUG), and tryptophan (Trp, UGG), showing values of RSCU = 1, most of the PEGs exhibited codon usage preference. By analyzing the RSCU of the mitogenome coding gene in *M. elegans*, it was shown that the RSCU values of 29 codons (e.g., AGA, CAA, and GGA) were more significant than 1 (Table S3), indicating a very high frequency of the relative usage. Interestingly, the alanine (GCU) has the highest codon usage preference (RSCU = 1.63), followed by the termination codon UAA (RSCU = 1.61), and leucine (Leu, RSCU = 1.60), showing a preference for UUA. By contrast, the proline (Pro) and threonine (Thr) had a higher RSCU value (>1.5) for CCU and ACU, respectively, indicating a solid codon usage bias. Notably, the glutamine (Gln, CAA), glycine (Gly, GGA), histidine (His, CAU), and serine (Ser, UCU) also have typical codon use preferences. However, the codon usage bias did not correlate with the tRNA copy numbers (Table 2).

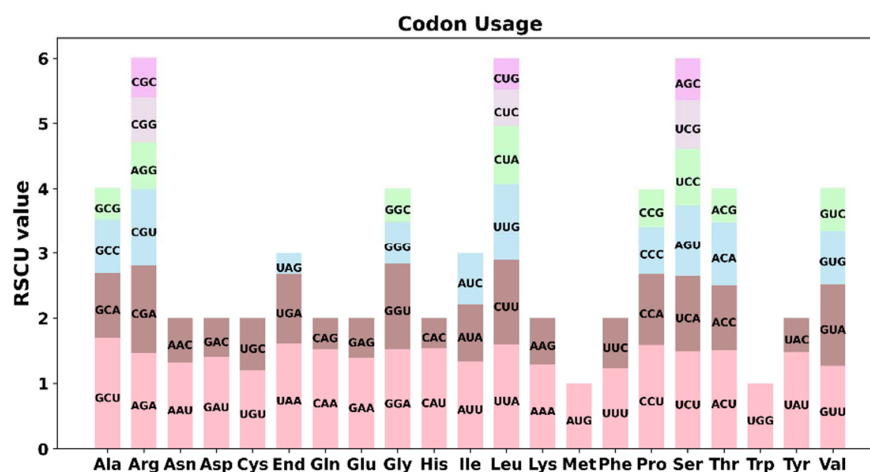


**Figure 3.** Analyses of the codon usage preference. X-axis, codon families for amino acids. Y-axis, RSCU value. RSCU, the relative synonymous codon usage.

### 3.3. Repetitive Sequences and the DNA Migration between Plastome and Mitogenome

Plenty of repeated sequences occurred in the plant mitogenome, including tandem and dispersed repeats. Simple sequence repeats (SSRs) are an uncommon tandem repeat with less than 6 bp length. Approximately 61 and 48 SSRs were identified in M1

and M2, primarily in the monomeric and dimeric forms, accounting for 52.46% and 68.75%, respectively. Analyses revealed the presence of one hexameric SSR (red color) and two pentameric SSRs (orange color) in M1 but not in M2 (Figure 4a, Tables S4 and S5). By contrast, the AG repeat was the most common type (76.19%) in dimeric SSRs. At least five tandem repeats (18–24 bp) with a match of more than 80% were detected in the mitogenome. Besides, a total of 232 (114 palindromic, 108 forward, four complementary, and reverse repeats) and 121 (62 palindromic, 58 forward, one complementary, and one reverse repeats) pairs of the dispersed repeat (>30 bp) were observed, showing distributions in M1 and M2, respectively (Figure 4b and Tables S6–S9). The longest palindromic repeat is 170 bp; in this case, the forward repeats showed a length of 197 bp.

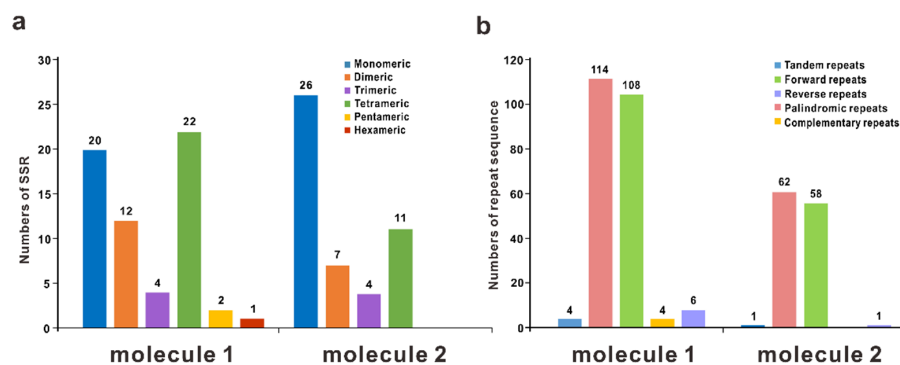


**Figure 4.** Analysis of the various sequence repeats in the mitogenome of the *M. elegans*. (a) The numbers and six types of SSR are shown in M1 and M2. (b) The detailed number of tandem repeats and four types of dispersed repeats (forward, reverse, palindromic, and complementary repeats) in M1 and M2. SSR, simple sequence repeat.

Based on Figure S1, the assembled complete plastome of the *M. elegans* was deciphered by high-throughput sequencing, revealing a length of 155,245 bp with a GC content of 37.4%, in line with a previous report [51]. Based on the sequence similarity, a total of 18 mitochondrial-to-plastid transfer points (MTPTs) with a total length of 8438 bp, accounting for 2.03% of the entire mitogenome, showed a sequence homology to that in the plastome (Figure 5). Both homologous DNA fragments, MTPT1 (M1) and MTPT2 (M2), had the most extended sequence length (2221 bp) compared to the others, ranging in length from 67 to 714 bp (Table S10). The annotation of MTPTs revealed the presence of seven intact genes, including a single PEG (*petG*) and six tRNA genes (*trnD-GUC*, *trnH-GUG*, *trnM-CAU*, *trnN-GUU*, *trnP-UGG*, and *trnW-CCA*). Besides, substantial long-reads were blasted to be spanned across the MTPTs (Tables S11 and S12).

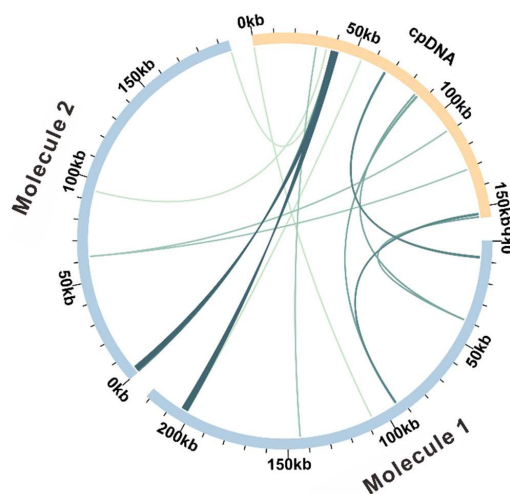


**Figure 5.** The gene transfers occurred between the plastome and mitogenome of *M. elegans*. The green ribbons connecting the arcs represent homologous segments transferred between the two organelles.

### 3.4. RNA Editing Events and Experimental Validation

RNA editing events occur commonly in the plant mitogenome, referring to the specific modification of the RNA sequence at particular sites. This rule creates RNA products that differ from DNA templates [52]. Recent advances in high-throughput sequencing technology have facilitated a more comprehensive survey of RNA editing patterns in plant mitogenomes [53]. Thirty-one unique PEGs annotated from the mitogenome in *M. elegans* were used to predict the RNA editing sites based on the PREP suite. Under the criteria (cutoff = 0.2), 350 RNA potential editing sites were identified with distributions on 31 mitochondrial PEGs, all of which were C-U/T edits (Figure 6 and Table S13). Most frequently, the *nad4* showed 31 RNA editing sites, followed by *ccmB*, containing 26 RNA editing sites. By contrast, one RNA edit was predicted in *atp8*, *rps7*, and *rps13*, whereas the *cox1* displayed the lowest RNA editing site count.

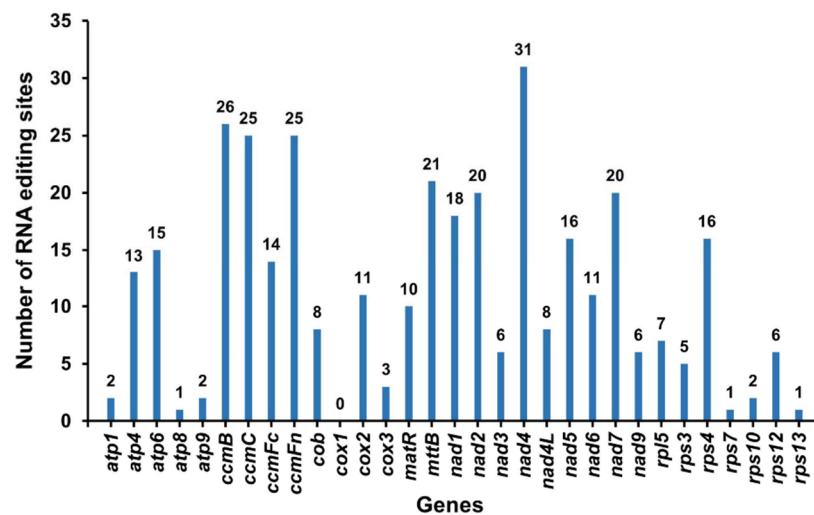


**Figure 6.** The number of RNA editing sites predicted in 31 PEGs.

Four essential structural PEGs (*cox2*, *nad1*, *nad7*, and *atp6*) in the mitogenome, comprising 16 predicted RNA editing sites (C-T), were randomly selected to verify the accuracy of RNA editing events predicted in the complete mitogenome of the *M. elegans*. The PCR amplification combined with Sanger sequencing assays was performed using DNA and complementary DNA (cDNA) as templates. The 16 selected RNA editing sites (e.g., *cox2*-243, *nad1*-215, *nad7*-224, and *atp6*-1015) were experimentally validated. Among them, twelve sites were successfully verified through PCR amplification of DNA and cDNA, accounting for 75% consistency in the prediction (Figure 7a,b and Table S14).

### 3.5. Sequence Colinearity and Phylogenetic Evolution

Based on the homologous analyses by MCscanX software, the multiple synteny plot revealed the collinearity patterns between eight plant mitogenomes within the order Caryophyllales (Table S15). The collinear blocks with sequence lengths less than 0.5 kb were not retained in the results. As shown in Figure 8a, the red curved ribbons indicate regions where the DNA inversion occurred, while the ribbons in gray represent the regions with a relatively high homology. Some blank regions identified were considered as individual blocks in a specific species. In addition, many homologous colinear blocks of short length were detected between the *M. elegans* and other genetically related species, prompting the insignificantly conserved relationship due to genome rearrangement and reorganization.

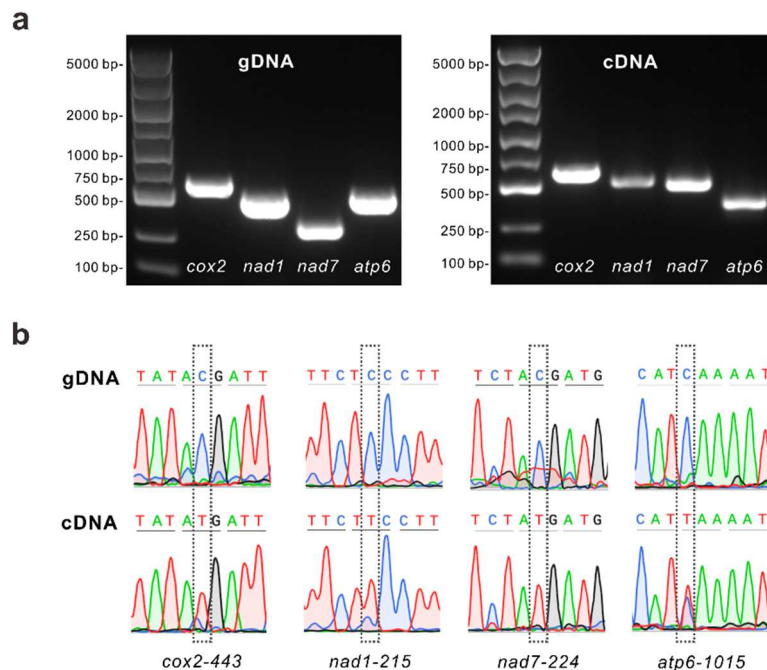


**Figure 7.** Experimental evaluation of the RNA editing sites in selected PEGs. (a) The amplified PCR production was performed using the gDNA and cDNA as templates. (b) A comparison of the RNA editing sites (*cox2*, *nad1*, *nad7*, and *atp6*) showed the C to U/T changes confirmed by the Sanger sequencing (dashed rectangles).

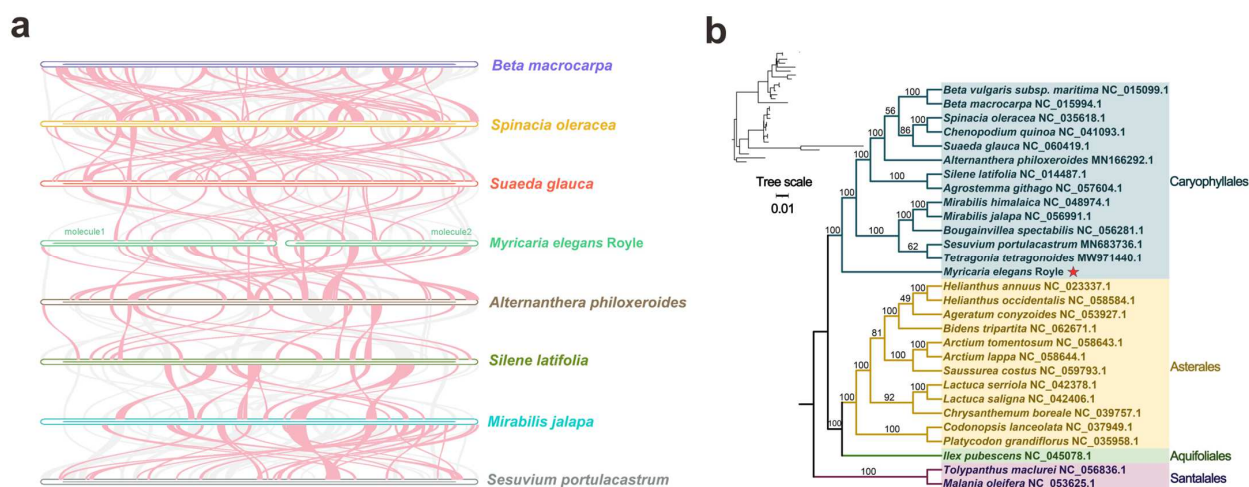


**Figure 8.** The evolutionary and collinearity analyses between *M. elegans* and other plant species. (a) Multiple synteny plot of the eight mitogenomes within order Caryophyllales. The ribbons depict the homologous sequences. The red highlights inversions that occurred, and the gray indicates regions with solid homology. (b) The neighbor-joining tree was constructed using complete mitogenomes of 29 genetically related species.

The subsequent evolutionary analyses were conducted using the available full-length mitogenomes of four selected orders (Caryophyllales, Asterales, Aquifoliales, and Santalales), comprising 29 plant species. The *Tolypanthus maclurei* (Merr.) Danser. and *Malania oleifera* Chun & S. K. Lee. in the order Santalales were used as an outgroup (Figure 8b). Approximately 18 PEGs shared conserved features in all selected species, including seven *nads* (*nad1*, 2, 3, 5, 6, 7, and 9), four *atps* (*atp1*, 4, 6, and 8), three *ccms* (*ccmC*, *ccmFc*, and *ccmFn*), two *coxs* (*cox2* and 3), *matR*, and *rps3*. The species classified into the same family were clustered together. The phylogenetic topology based on the com-

plete mitogenome coincides with the latest Angiosperm Phylogeny Group (APG) system classification. Based on the evolutionary tree, the *M. elegans* in the subclade of the family Tamaricaceae was identified in the basal position of the order Caryophyllales.

#### 4. Discussion

*Myricaria* species occur majorly in or around the high-altitude Qinghai–Tibetan Plateau and the Himalayan mountains within Eurasia, except for the *M. laxiflora* (Franch.) P. Y. Zhang & Y. J. Zhang. Most are critical ecological and pharmaceutical resources [3]. By contrast, the *M. elegans* species is an ethnobotanical herb and grows at the riverside and arid areas of the highest altitude mountains (>3500 m), exhibiting superior qualities in extreme climate tolerance and tangible economic benefits to indigenous communities in poverty [4]. Despite its versatile potentialities, the *M. elegans* species remains overlooked and underutilized owing to the lack of molecular backgrounds in genetic and evolutionary diversities. In this study, using the short-read (Illumina) and long-read (PacBio) sequencing data, the complete mitogenome of the *M. elegans* was assembled and annotated, showing a total length of 416,354 bp, with GC content of 44.33% and 31 unique PEGs. Our data demonstrate that the representation of the mitogenome in the genus *Myricaria* is not a single linear form and that, in reality, it is a complex, dynamic conformation and mixture of two circular molecules (Figures 1 and 2).

Extensive genomic rearrangements were identified in the mitogenome of the *M. elegans* and the genetically related species, while the PEGs were highly conserved. High-throughput sequencing technologies have revolutionized the field of genomics, enabling the efficient and cost-effective assembly of the complete mitogenome [11]. Exploring the mitogenome of *M. elegans* will contribute to a comprehensive understanding of its genetic makeup and facilitate future research endeavors to unravel the mechanisms underlying its high adaptability and valuable traits. This study enriches the genetic information for the order Caryophyllales, providing a theoretical clue for improving germplasm development and biological conservation in western Tibet, China.

Plant photosynthesis and respiration are the essential tools driving energy acquisition, biomass, and other crucial physiological processes modulated by plastids and mitochondria [54]. Mitochondria, as a critical organelle in eukaryotic cells, is a semi-autonomous organelle, encoding structural genes related to their functions and participating in some processes of life activities, and closely related to plant cytoplasmic male sterility and species evolution [55]. For most land plants, mitogenomes are maternally inherited, which simplifies evolutionary plasticity and has been widely attempted to infer in-depth phylogenetic relationships in the taxonomy and conservation [56,57]. The more prominent mitogenomes in plants exhibit lower mutation rates and more rearrangements than in animals [58]. Nevertheless, a more significant variation and diversity in mitochondrial structural genes and intron contents occurred across the eukaryotes, indicating the massive convergent evolution [59].

During the past decades, technological advances in genome sequencing have contributed to a meteoric rise in published organellar genomes, revealing significantly divergent evolutionary trajectories [22]. The assembly and reporting of complete plant mitogenomes are continually increasing, with an increasing number of mitogenomes employed in studies related to germplasm identification, phylogenies, and other areas. The prolonged endo-symbiotic origin of the mitochondria led to the loss of some original DNA, with only DNA encoding essential functions remaining due to transfers [60]. The evolutionary analysis through a comparative analysis of mitogenomes unraveled the genetic variation, structure, and diversity in rice and *S. glauca* [16,61]. The unique patterns of plant mitogenomes, including compactness, high copy number, and frequent rearrangements, reflect the complex evolutionary history and ongoing ecological adaptation to the critical environment cues [62]. Thus, understanding typical features of mitogenomes is crucial for unraveling plant functional significance and evolutionary patterns.

The mitogenome is regarded as an entity with dynamic changes during evolution, displaying substantial variation in size and structure within various plant species [63]. Many repeat sequences and exogenous sequence insertions were identified in plant mitogenomes, leading to gene loss, multiple copies, and genomic rearrangements mediating the form of the multi-branched conformation [64]. Understanding the mitogenome structure is required to unravel its function, replication, inheritance, and evolutionary trajectories [12]. In this study, a hybrid assembly strategy was employed, combining Illumina short-read and PacBio long-read sequencing assays to decipher the mitogenome of the *M. elegans*. Functional genes are often imbalanced across molecules in plant multi-branched mitogenomes, resulting in the absence of functional genes on numerous molecules [26]. The comparative analysis revealed the conservation of mitogenome size and gene contents, albeit with complex genome structures. Among the 41 standard PEGs from the mitogenome of the common ancestor in angiosperms, thirty-one structural genes were annotated in the *M. elegans* mitogenome, including 24 mitochondrial core genes and 7 non-core genes, implicating that lost genes might be due to the transfer into the nuclear genome, a common phenomenon during a long-term evolution in angiosperm [65]. Further, transcriptomic sequencing and *in vivo* compartmental analyses are needed to determine whether these genes can be expressed explicitly in the plant mitochondria.

The codons are the primary carriers, providing accurate translation and transmission of genetic information in nature that plays a crucial role in biological genetics and variation [66]. Principally, except for Met and Trp, all of the 20 amino acids that constitute natural proteins correspond to 2–6 synonymous codons. The selection and use of synonymous codons do not alter the amino acid, which is beneficial for translation accuracy but may impact protein expression levels [67]. The differences for individual amino acids in the frequency of the codon usage were predicted, prompting the codon usage preference among 31 PEGs in the mitogenome of the *M. elegans* (Figure 3). Based on the prediction, 29 codons showed RSCU values of more than 1, including 13 codons ending in A, 16 codons ending in U, and 1 termination codon in G, reflecting the constant evolution trend of base composition. Even though the correlation between the codon usage preferences and annotated tRNAs and gene copy numbers was not set up, it may be due to semi-autonomous protein biosynthesis and metabolism in the mitochondria. This finding fits well with early research on codon usage preference in soybeans [68]. These results provide an essential reference for codon optimization of exogenous genes in the next step, thereby enhancing the protein expression.

The mitogenome encompasses a diverse repertoire of repetitive DNA sequences (repeats), encompassing tandem repeats, short reiterated motifs, and substantial duplications [29]. Previous reports have unveiled the intrinsic significance of repeats within mitogenome, as they play an irreplaceable role in promoting intermolecular recombination mechanisms [11]. Consequently, these reiterated sequences are paramount in shaping the mitogenome, profoundly influencing its structural and functional dynamics [69]. In this study, the SSRs, long tandem repeats, and dispersed repeats were intensively investigated (Figure 3). The mitogenome of *M. elegans* harbors abundant sequence repeats, inferring that intermolecular recombination frequently alters the sequence size and conformation dynamically during the evolution. The results showed that all four pairs of repetitive sequences, 44, 48, 45, and 28, had long-reads supporting recombination conformation. For the most extended repeat sequence, a 20 kb, 14-22-7 MTPTs, similar to the plastid inverted repeat (IR) region, usually mediate recombination at nearly 50%. However, sequence repeats do not necessarily affect genomic recombination, particularly for shorter reads, so only long-reads were used for validation. Experimental validation can be performed for longer segments of the repeats by designing primers using PCR at the repeat sequence boundaries.

As migration of plastidic DNA to the mitogenome occurred during the evolution, the transfer of tRNA genes is regarded as a joint event in angiosperms [70]. Many MTPTs initially identified in the mitogenome have been lost during the evolution, which is related to functional adaptation [28]. The *sdh2* encoding succinate dehydrogenase was identified

as the loss in the early evolution of the plant mitogenomes, and *rps9*, 11, and 16 are not present evenly in various plant kingdoms [71]. Besides, the *rps12*, *sdh3*, and *sdh4* were not characterized in rice mitogenome, but the *rps2* appeared to happen in monocots merely [21]. This study observed 18 MTPs originating from the plastome, prompting the conserved transfer and evolutionary diversity, which resulted in the integration and recombination of seven PEGs (Figure 5). The exogenous genes encompassed one PEG and six tRNA genes, accounting for 10.3% DNA transfer between plastome and mitogenome, which was in concert with the findings [72].

Innovations in DNA/RNA-sequencing techniques have dramatically increased the number of genomes and transcriptomes released, thus providing vital clues on RNA editing for numerous plant organisms. RNA editing events follow post-transcriptional mechanisms in the plastome and mitogenome, an enigmatic reaction in RNA levels that maintains normal biological function and fine-tuned protein folding in flowering plants [52]. The primary type of RNA editing is the conversion of C-U, occasionally accompanied by U-C conversions [73]. Previous reports in cotton revealed that RNA editing in a mitochondrial gene (*atp1*) affects ATP production and the elongation of trichome and fibers [74]. The dosage in RNA editing sites can lead to significant changes in the RNA sequence rewritten, affecting the translation process, protein structure, and interactions between the mitogenome and nuclear genome [75]. In *Arabidopsis*, 441 RNA editing sites were deduced in mitogenome with distribution in 36 PEGs [75]. In a model monocot of rice mitogenome, approximately 491 RNA editing sites were identified for the occurrence in 34 PEGs [21]. Recently, the mitogenome of a halophyte species (*S. glauca*) revealed 216 RNA editing sites predicted in 26 PEGs [16]. In our work, the prediction of 31 PEGs in the mitogenome of *M. elegans* suggested that 350 RNA editing sites occurred, of which the *nad4*, encoding the NADH dehydrogenase, ranked the highest number (Figure 8 and Table S13). As *nad4* encodes the central subunit of the mitochondrial respiratory chain complex I, it plays an essential role in respiration and ATP synthesis [76]. Therefore, the increased RNA editing sites in *nad4* may reflect the critical nature of regulating oxidative phosphorylation and cellular metabolism. Interestingly, only one RNA editing site was identified in three PEGs (*atp8*, *rps7*, and *rps13*), indicating retained sequence variation and conserved patterns during evolution. Fewer RNA editing events in specific genes were postulated to be important in their functional adaptation and structure maintenance, particularly at the post-transcriptional level [52].

Furthermore, the synteny analyses revealed that the mitogenome of *M. elegans* has relatively good co-linear blocks but a non-conservative link with other species within Caryophyllales, indicating that they underwent extensive genome rearrangement during the evolution (Figure 8). In addition, the phylogenetic relationship was determined using complete mitogenomes of four representative orders, including *M. elegans* and other species. The resulting unrooted trees reflected well-defined taxonomic relationships between different orders. In contrast, the *M. elegans* evolved more anciently in the order Caryophyllales, clustering the original feature and clues that additional mitogenomic information is needed to flourish the genus *Myricaria*, Tamaricaceae pools.

## 5. Conclusions

The comprehensive mitogenome assembly and annotation were implemented using advanced techniques to capture the spectrum of gene isoforms, leading to an extensive inference of mitogenomic structures and recombination activities in *M. elegans*. In this study, we aimed to decipher the extensive mitogenome of *M. elegans* using the combined high-throughput sequencing assays (e.g., Illumina and PacBio) and bioinformatics approaches. The elucidated mitogenome of genus *Myricaria* contributes to comprehensively understanding its dynamic conformation, genome reorganization, DNA migration, and RNA editing events, identifying potential functional conserved elements related to transcriptional modulation. The availability of the mitogenome facilitates future studies on the genetic evolution, phylogenies, and biological conservation of the *M. elegans*, family Tamaricaceae. Therefore, unraveling mitochondrial molecular background has implications for ecological benefits,

economic efforts, and developing strategies for enhancing the saline-drought tolerance and pharmaceutical use of halophytes in high-altitude mountains. By orchestrating the genetic frame of the Plateau Hongliu in western Tibet, our work provides insights into the theoretical basis for their climate resilience and adaptation in extremely arid areas.

**Supplementary Materials:** The following supporting information can be downloaded at: <https://www.mdpi.com/article/10.3390/f15050835/s1>, File S1 includes Supplementary Figures and Tables. Figure S1: The plastid genome map and gene annotations of the *M. elegans*. Table S1: Statistics of the mitogenome assembly in *M. elegans*; Table S2: Basic information of *M. elegans* mitogenome. Table S3: Relative synonymous codon usage in *M. elegans* mitogenome; Table S4: SSRs in the mitogenome of M1; Table S5: SSRs in the mitogenome of M2; Table S6: Tandem repeat sequences in the mitogenome of M1; Table S7: Tandem repeat sequences in the mitogenome of *M. elegans*; Table S8: Dispersed repeats sequences in M1; Table S9: Dispersed repeats sequences in the mitogenome of M2; Table S10: The homologous DNA fragment in the *M. elegans* mitogenome; Table S11: The collection of long-reads obtained from BLASTn results that can support different paths; Table S12: Potential paths and the number of long-reads; Table S13: RNA editing in *M. elegans* mitogenome; Table S14: Primer sequences used for RNA editing evaluation. Table S15: The NCBI accession numbers of all used plant mitogenomes. File S2: Sanger sequencing data for the RNA editing sites validation.

**Author Contributions:** X.L., H.W. and X.H.: Conceptualization, Investigation, Formal analysis, and Writing—original draft; Y.W. and F.N.: Resources, Formal analysis, Data curation, and Software. T.S. and M.H.: Conceptualization, Supervision, Project administration, and Writing—review & editing. F.C.: Funding acquisition, Supervision, and Writing—review & editing. All authors have read and agreed to the published version of the manuscript.

**Funding:** This research was funded by the National Key Technology Research and Development Program (NKTRDP) (2022YFD2200601), the Postgraduate Research & Practice Innovation Program of Jiangsu Province (PRPIPJP) (SJCX22\_0329), the National Natural Science Foundation of China (NSFJ) (31870589), and the Natural Science Foundation of Jiangsu Province (NSFJ) (BK20170921).

**Data Availability Statement:** In this study, the generated *M. elegans* mitogenome sequences were submitted to the GenBank database with the accession ID OP429117 (M1) and OP429118 (M2). The SRA numbers are available for the raw data at GenBank database with the SRA ID: SRR28705194, Illumina (<https://www.ncbi.nlm.nih.gov/sra/SRR28705194>, accessed on 16 April 2024) and SRR28705193, PacBio (<https://www.ncbi.nlm.nih.gov/sra/SRR28705193>, accessed on 16 April 2024).

**Acknowledgments:** The authors would like to thank all funding agencies (NKTRDP, PRPIPJP, NSFJ, and NSFJ) for supporting this work. Our thanks go to the Co-Innovation Center for Sustainable Forestry in Southern China, the State Key Laboratory of Tree Genetics and Breeding, and the Priority Academic Program Development of Jiangsu Higher Education Institutions for using instruments.

**Conflicts of Interest:** The authors declare no conflicts of interest.

## References

- Zhang, M.-L.; Meng, H.-H.; Zhang, H.-X.; Vyacheslav, B.V.; Sanderson, S.C. Himalayan Origin and Evolution of Myricaria (Tamaricaceae) in the Neogene. *PLoS ONE* **2014**, *9*, e97582. [[CrossRef](#)]
- Dolezal, J.; Kopecky, M.; Dvorsky, M.; Macek, M.; Rehakova, K.; Capkova, K.; Borovec, J.; Schweingruber, F.; Liancourt, P.; Altman, J. Sink limitation of plant growth determines tree line in the arid Himalayas. *Funct. Ecol.* **2019**, *33*, 553–565. [[CrossRef](#)]
- Hu, H.; Wang, Q.; Hao, G.; Zhou, R.; Luo, D.; Cao, K.; Yan, Z.; Wang, X. Insights into the phylogenetic relationships and species boundaries of the *Myricaria squamosa* complex (Tamaricaceae) based on the complete chloroplast genome. *PeerJ* **2023**, *11*, e16642. [[CrossRef](#)]
- Haq, S.M.; Yaqoob, U.; Calixto, E.S.; Rahman, I.U.; Hashem, A.; Abd\_Allah, E.F.; Alakeel, M.A.; Alqarawi, A.A.; Abdalla, M.; Hassan, M.; et al. Plant Resources Utilization among Different Ethnic Groups of Ladakh in Trans-Himalayan Region. *Biology* **2021**, *10*, 827. [[CrossRef](#)]
- Khan, S.; Nisar, M.; Khan, R.; Ahmad, W.; Nasir, F. Evaluation of Chemical Constituents and Antinociceptive Properties of *Myricaria elegans* Royle. *Chem. Biodivers.* **2010**, *7*, 2897–2900. [[CrossRef](#)]
- Archibald, J.M. Endosymbiosis and Eukaryotic Cell Evolution. *Curr. Biol.* **2015**, *25*, R911–R921. [[CrossRef](#)]
- Kummer, E.; Ban, N. Mechanisms and regulation of protein synthesis in mitochondria. *Nat. Rev. Mol. Cell Biol.* **2021**, *22*, 307–325. [[CrossRef](#)]

8. Ghifari, A.S.; Saha, S.; Murcha, M.W. The biogenesis and regulation of the plant oxidative phosphorylation system. *Plant Physiol.* **2023**, *192*, 728–747. [[CrossRef](#)]
9. Munasinghe, M.; Ågren, J.A. When and why are mitochondria paternally inherited? *Curr. Opin. Genet. Dev.* **2023**, *80*, 102053. [[CrossRef](#)]
10. Møller, I.M.; Rasmusson, A.G.; Van Aken, O. Plant mitochondria—past, present and future. *Plant J.* **2021**, *108*, 912–959. [[CrossRef](#)]
11. Sloan, D.B. One ring to rule them all? Genome sequencing provides new insights into the ‘master circle’ model of plant mitochondrial DNA structure. *New Phytol.* **2013**, *200*, 978–985. [[CrossRef](#)] [[PubMed](#)]
12. Kozik, A.; Rowan, B.A.; Lavelle, D.; Berke, L.; Eric Schranz, M.; Michelmore, R.W.; Christensen, A.C. The alternative reality of plant mitochondrial DNA: One ring does not rule them all. *PLoS Genet.* **2019**, *15*, 1–30. [[CrossRef](#)] [[PubMed](#)]
13. Zhou, S.; Zhi, X.; Yu, R.; Liu, Y.; Zhou, R. Factors contributing to mitogenome size variation and a recurrent intracellular DNA transfer in *Melastoma*. *BMC Genom.* **2023**, *24*, 370. [[CrossRef](#)] [[PubMed](#)]
14. Bi, C.; Sun, N.; Han, F.; Xu, K.; Yang, Y.; Ferguson, D.K. The first mitogenome of Lauraceae (*Cinnamomum chekiangense*). *Plant Divers.* **2024**, *46*, 144–148. [[CrossRef](#)] [[PubMed](#)]
15. Unseld, M.; Marienfeld, J.R.; Brandt, P.; Brennicke, A. The mitochondrial genome of *Arabidopsis thaliana* contains 57 genes in 366,924 nucleotides. *Nat. Genet.* **1997**, *15*, 57–61. [[CrossRef](#)]
16. Cheng, Y.; He, X.; Priyadarshani, S.V.G.N.; Wang, Y.; Ye, L.; Shi, C.; Ye, K.; Zhou, Q.; Luo, Z.; Deng, F.; et al. Assembly and comparative analysis of the complete mitochondrial genome of *Suaeda glauca*. *BMC Genom.* **2021**, *22*, 167. [[CrossRef](#)] [[PubMed](#)]
17. Alverson, A.J.; Wei, X.; Rice, D.W.; Stern, D.B.; Barry, K.; Palmer, J.D. Insights into the Evolution of Mitochondrial Genome Size from Complete Sequences of *Citrullus lanatus* and *Cucurbita pepo* (Cucurbitaceae). *Mol. Biol. Evol.* **2010**, *27*, 1436–1448. [[CrossRef](#)] [[PubMed](#)]
18. Chang, S.; Wang, Y.; Lu, J.; Gai, J.; Li, J.; Chu, P.; Guan, R.; Zhao, T. The Mitochondrial Genome of Soybean Reveals Complex Genome Structures and Gene Evolution at Intercellular and Phylogenetic Levels. *PLoS ONE* **2013**, *8*, e56502.
19. Handa, H. The complete nucleotide sequence and RNA editing content of the mitochondrial genome of rapeseed (*Brassica napus* L.): Comparative analysis of the mitochondrial genomes of rapeseed and *Arabidopsis thaliana*. *Nucleic Acids Res.* **2003**, *31*, 5907–5916. [[CrossRef](#)]
20. Ogiwara, Y. Structural dynamics of cereal mitochondrial genomes as revealed by complete nucleotide sequencing of the wheat mitochondrial genome. *Nucleic Acids Res.* **2005**, *33*, 6235–6250. [[CrossRef](#)]
21. Notsu, Y.; Masood, S.; Nishikawa, T.; Kubo, N.; Akiduki, G.; Nakazono, M.; Hirai, A.; Kadowaki, K. The complete sequence of the rice (*Oryza sativa* L.) mitochondrial genome: Frequent DNA sequence acquisition and loss during the evolution of flowering plants. *Mol. Genet. Genom.* **2002**, *268*, 434–445. [[CrossRef](#)] [[PubMed](#)]
22. Jiang, M.; Ni, Y.; Zhang, J.; Li, J.; Liu, C. Complete mitochondrial genome of *Mentha spicata* L. reveals multiple chromosomal configurations and RNA editing events. *Int. J. Biol. Macromol.* **2023**, *251*, 126257. [[CrossRef](#)]
23. Richardson, A.O.; Rice, D.W.; Young, G.J.; Alverson, A.J.; Palmer, J.D. The “fossilized” mitochondrial genome of *Liriodendron tulipifera*: Ancestral gene content and order, ancestral editing sites, and extraordinarily low mutation rate. *BMC Biol.* **2013**, *11*, 29. [[CrossRef](#)] [[PubMed](#)]
24. Skippington, E.; Barkman, T.J.; Rice, D.W.; Palmer, J.D. Miniaturized mitogenome of the parasitic plant *Viscum scurruloideum* is extremely divergent and dynamic and has lost all nad genes. *Proc. Natl. Acad. Sci. USA* **2015**, *112*, E3515–E3524. [[CrossRef](#)] [[PubMed](#)]
25. Sloan, D.B.; Alverson, A.J.; Chuckalovcak, J.P.; Wu, M.; McCauley, D.E.; Palmer, J.D.; Taylor, D.R. Rapid Evolution of Enormous, Multichromosomal Genomes in Flowering Plant Mitochondria with Exceptionally High Mutation Rates. *PLoS Biol.* **2012**, *10*, e1001241. [[CrossRef](#)] [[PubMed](#)]
26. Wu, Z.; Liao, X.; Zhang, X.; Tembrock, L.R.; Broz, A. Genomic architectural variation of plant mitochondria—A review of multichromosomal structuring. *J. Syst. Evol.* **2022**, *60*, 160–168. [[CrossRef](#)]
27. Shtolz, N.; Mishmar, D. The Mitochondrial Genome—on Selective Constraints and Signatures at the Organism, Cell, and Single Mitochondrion Levels. *Front. Ecol. Evol.* **2019**, *7*, 342. [[CrossRef](#)]
28. Lei, B.; Li, S.; Liu, G.; Chen, Z.; Su, A.; Li, P.; Li, Z.; Hua, J. Evolution of mitochondrial gene content: Loss of genes, tRNAs and introns between *Gossypium harknessii* and other plants. *Plant Syst. Evol.* **2013**, *299*, 1889–1897. [[CrossRef](#)]
29. Grewe, F.; Viehoveer, P.; Weisshaar, B.; Knooper, V. A trans-splicing group I intron and tRNA-hyperediting in the mitochondrial genome of the lycophyte *Isoetes engelmannii*. *Nucleic Acids Res.* **2009**, *37*, 5093–5104. [[CrossRef](#)]
30. Tong, W.; Kim, T.-S.; Park, Y.-J. Rice Chloroplast Genome Variation Architecture and Phylogenetic Dissection in Diverse *Oryza* Species Assessed by Whole-Genome Resequencing. *Rice* **2016**, *9*, 57. [[CrossRef](#)]
31. Arseneau, J.; Steeves, R.; Laflamme, M. Modified low-salt CTAB extraction of high-quality DNA from contaminant-rich tissues. *Mol. Ecol. Resour.* **2017**, *17*, 686–693. [[CrossRef](#)] [[PubMed](#)]
32. Jin, J.-J.; Yu, W.-B.; Yang, J.-B.; Song, Y.; DePamphilis, C.W.; Yi, T.-S.; Li, D.-Z. GetOrganelle: A fast and versatile toolkit for accurate de novo assembly of organelle genomes. *Genome Biol.* **2020**, *21*, 241. [[CrossRef](#)] [[PubMed](#)]
33. Wick, R.R.; Schultz, M.B.; Zobel, J.; Holt, K.E. Bandage: Interactive visualization of de novo genome assemblies. *Bioinformatics* **2015**, *31*, 3350–3352. [[CrossRef](#)] [[PubMed](#)]
34. Li, H.; Durbin, R. Fast and accurate short read alignment with Burrows–Wheeler transform. *Bioinformatics* **2009**, *25*, 1754–1760. [[CrossRef](#)] [[PubMed](#)]

35. Tillich, M.; Lehwork, P.; Pellizzer, T.; Ulbricht-Jones, E.S.; Fischer, A.; Bock, R.; Greiner, S. GeSeq—versatile and accurate annotation of organelle genomes. *Nucleic Acids Res.* **2017**, *45*, W6–W11. [[CrossRef](#)] [[PubMed](#)]
36. Chan, P.P.; Lin, B.Y.; Mak, A.J.; Lowe, T.M. tRNAscan-SE 2.0: Improved detection and functional classification of transfer RNA genes. *Nucleic Acids Res.* **2021**, *49*, 9077–9096. [[CrossRef](#)] [[PubMed](#)]
37. Chen, Y.; Ye, W.; Zhang, Y.; Xu, Y. High speed BLASTN: An accelerated MegaBLAST search tool. *Nucleic Acids Res.* **2015**, *43*, 7762–7768. [[CrossRef](#)] [[PubMed](#)]
38. Zhang, D.; Gao, F.; Jakovlić, I.; Zou, H.; Zhang, J.; Li, W.X.; Wang, G.T. PhyloSuite: An integrated and scalable desktop platform for streamlined molecular sequence data management and evolutionary phylogenetics studies. *Mol. Ecol. Resour.* **2020**, *20*, 348–355. [[CrossRef](#)] [[PubMed](#)]
39. Kumar, S.; Stecher, G.; Li, M.; Knyaz, C.; Tamura, K. MEGA X: Molecular Evolutionary Genetics Analysis across Computing Platforms. *Mol. Biol. Evol.* **2018**, *35*, 1547–1549. [[CrossRef](#)]
40. Benson, G. Tandem repeats finder: A program to analyze DNA sequences. *Nucleic Acids Res.* **1999**, *27*, 573–580. [[CrossRef](#)]
41. Kurtz, S. REPuter: The manifold applications of repeat analysis on a genomic scale. *Nucleic Acids Res.* **2001**, *29*, 4633–4642. [[CrossRef](#)] [[PubMed](#)]
42. Zhang, H.; Meltzer, P.; Davis, S. RCircos: An R package for Circos 2D track plots. *BMC Bioinform.* **2013**, *14*, 244. [[CrossRef](#)] [[PubMed](#)]
43. Shi, L.; Chen, H.; Jiang, M.; Wang, L.; Wu, X.; Huang, L.; Liu, C. CPGAVAS2, an integrated plastome sequence annotator and analyzer. *Nucleic Acids Res.* **2019**, *47*, W65–W73. [[CrossRef](#)]
44. Chen, C.; Chen, H.; Zhang, Y.; Thomas, H.R.; Frank, M.H.; He, Y.; Xia, R. TBtools: An Integrative Toolkit Developed for Interactive Analyses of Big Biological Data. *Mol. Plant* **2020**, *13*, 1194–1202. [[CrossRef](#)]
45. Milne, I.; Stephen, G.; Bayer, M.; Cock, P.J.A.; Pritchard, L.; Cardle, L.; Shaw, P.D.; Marshall, D. Using Tablet for visual exploration of second-generation sequencing data. *Brief. Bioinform.* **2013**, *14*, 193–202. [[CrossRef](#)] [[PubMed](#)]
46. Mower, J.P. The PREP suite: Predictive RNA editors for plant mitochondrial genes, chloroplast genes and user-defined alignments. *Nucleic Acids Res.* **2009**, *37*, W253–W259. [[CrossRef](#)]
47. Wang, Y.; Tang, H.; DeBarry, J.D.; Tan, X.; Li, J.; Wang, X.; Lee, T.-H.; Jin, H.; Marler, B.; Guo, H.; et al. MCScanX: A toolkit for detection and evolutionary analysis of gene synteny and collinearity. *Nucleic Acids Res.* **2012**, *40*, e49. [[CrossRef](#)]
48. Katoh, K.; Standley, D.M. MAFFT Multiple Sequence Alignment Software Version 7: Improvements in Performance and Usability. *Mol. Biol. Evol.* **2013**, *30*, 772–780. [[CrossRef](#)]
49. Huelsenbeck, J.P.; Ronquist, F. MRBAYES: Bayesian inference of phylogenetic trees. *Bioinformatics* **2001**, *17*, 754–755. [[CrossRef](#)]
50. Letunic, I.; Bork, P. Interactive Tree Of Life (iTOL) v4: Recent updates and new developments. *Nucleic Acids Res.* **2019**, *47*, W256–W259. [[CrossRef](#)]
51. Han, M.; Xu, M.; Wang, S.; Wu, L.; Shi, Y.; Su, T. The complete chloroplast genome sequence of *Myricaria elegans*: An endemic species to the Himalayas. *Mitochondrial DNA Part B* **2021**, *6*, 3343–3345. [[CrossRef](#)] [[PubMed](#)]
52. Small, I.D.; Schallenberg-Rüdinger, M.; Takenaka, M.; Mireau, H.; Ostersetzer-Biran, O. Plant organellar RNA editing: What 30 years of research has revealed. *Plant J.* **2020**, *101*, 1040–1056. [[CrossRef](#)] [[PubMed](#)]
53. Guo, S.; Li, Z.; Li, C.; Liu, Y.; Liang, X.; Qin, Y. Assembly and characterization of the complete mitochondrial genome of *Ventilago leiocarpa*. *Plant Cell Rep.* **2024**, *43*, 77. [[CrossRef](#)] [[PubMed](#)]
54. Raven, J.A. Implications of mutation of organelle genomes for organelle function and evolution. *J. Exp. Bot.* **2015**, *66*, 5639–5650. [[CrossRef](#)] [[PubMed](#)]
55. Chen, Z.; Zhao, N.; Li, S.; Grover, C.E.; Nie, H.; Wendel, J.F.; Hua, J. Plant Mitochondrial Genome Evolution and Cytoplasmic Male Sterility. *CRC Crit. Rev. Plant Sci.* **2017**, *36*, 55–69. [[CrossRef](#)]
56. Yang, T.; Xu, G.; Gu, B.; Shi, Y.; Mzuka, H.L.; Shen, H. The Complete Mitochondrial Genome Sequences of the *Philomyces bilineatus* (Stylommatophora: Philomycidae) and Phylogenetic Analysis. *Genes* **2019**, *10*, 198. [[CrossRef](#)] [[PubMed](#)]
57. Ladoukakis, E.D.; Zouros, E. Evolution and inheritance of animal mitochondrial DNA: Rules and exceptions. *J. Biol. Res.* **2017**, *24*, 2. [[CrossRef](#)] [[PubMed](#)]
58. Darracq, A.; Varré, J.-S.; Touzet, P. A scenario of mitochondrial genome evolution in maize based on rearrangement events. *BMC Genom.* **2010**, *11*, 233. [[CrossRef](#)] [[PubMed](#)]
59. Mower, J.P. Variation in protein gene and intron content among land plant mitogenomes. *Mitochondrion* **2020**, *53*, 203–213. [[CrossRef](#)]
60. Knoop, V. The mitochondrial DNA of land plants: Peculiarities in phylogenetic perspective. *Curr. Genet.* **2004**, *46*, 123–139. [[CrossRef](#)]
61. Tong, W.; He, Q.; Park, Y.-J. Genetic variation architecture of mitochondrial genome reveals the differentiation in Korean landrace and weedy rice. *Sci. Rep.* **2017**, *7*, 43327. [[CrossRef](#)]
62. Taanman, J.-W. The mitochondrial genome: Structure, transcription, translation and replication. *Biochim. Biophys. Acta Bioenerg.* **1999**, *1410*, 103–123. [[CrossRef](#)] [[PubMed](#)]
63. Bi, C.; Qu, Y.; Hou, J.; Wu, K.; Ye, N.; Yin, T. Deciphering the Multi-Chromosomal Mitochondrial Genome of *Populus simonii*. *Front. Plant Sci.* **2022**, *13*, 914635. [[CrossRef](#)] [[PubMed](#)]
64. Gualberto, J.M.; Newton, K.J. Plant Mitochondrial Genomes: Dynamics and Mechanisms of Mutation. *Annu. Rev. Plant Biol.* **2017**, *68*, 225–252. [[CrossRef](#)] [[PubMed](#)]

65. McCauley, D.E. Paternal leakage, heteroplasmy, and the evolution of plant mitochondrial genomes. *New Phytol.* **2013**, *200*, 966–977. [[CrossRef](#)] [[PubMed](#)]
66. Hia, F.; Takeuchi, O. The effects of codon bias and optimality on mRNA and protein regulation. *Cell. Mol. Life Sci.* **2021**, *78*, 1909–1928. [[CrossRef](#)] [[PubMed](#)]
67. Radrizzani, S.; Kudla, G.; Izsvák, Z.; Hurst, L.D. Selection on synonymous sites: The unwanted transcript hypothesis. *Nat. Rev. Genet.* **2024**. [[CrossRef](#)] [[PubMed](#)]
68. Campbell, W.H.; Gowri, G. Codon Usage in Higher Plants, Green Algae, and Cyanobacteria. *Plant Physiol.* **1990**, *92*, 1–11. [[CrossRef](#)] [[PubMed](#)]
69. Zardoya, R. Recent advances in understanding mitochondrial genome diversity. *F1000Research* **2020**, *9*, 270. [[CrossRef](#)]
70. Turmel, M.; Lopes dos Santos, A.; Otis, C.; Sergerie, R.; Lemieux, C. Tracing the Evolution of the Plastome and Mitogenome in the Chloropicophyceae Uncovered Convergent tRNA Gene Losses and a Variant Plastid Genetic Code. *Genome Biol. Evol.* **2019**, *11*, 1275–1292. [[CrossRef](#)]
71. Ala, K.G.; Zhao, Z.; Ni, L.; Wang, Z. Comparative analysis of mitochondrial genomes of two alpine medicinal plants of Gentiana (Gentianaceae). *PLoS ONE* **2023**, *18*, e0281134. [[CrossRef](#)] [[PubMed](#)]
72. Sloan, D.B.; Wu, Z. History of Plastid DNA Insertions Reveals Weak Deletion and AT Mutation Biases in Angiosperm Mitochondrial Genomes. *Genome Biol. Evol.* **2014**, *6*, 3210–3221. [[CrossRef](#)] [[PubMed](#)]
73. Gerke, P.; Szövényi, P.; Neubauer, A.; Lenz, H.; Gutmann, B.; McDowell, R.; Small, I.; Schallenberg-Rüdinger, M.; Knoop, V. Towards a plant model for enigmatic U-to-C RNA editing: The organelle genomes, transcriptomes, editomes and candidate RNA editing factors in the hornwort *Anthoceros agrestis*. *New Phytol.* **2020**, *225*, 1974–1992. [[CrossRef](#)] [[PubMed](#)]
74. He, P.; Xiao, G.; Liu, H.; Zhang, L.; Zhao, L.; Tang, M.; Huang, S.; An, Y.; Yu, J. Two pivotal RNA editing sites in the mitochondrial atp1 mRNA are required for ATP synthase to produce sufficient ATP for cotton fiber cell elongation. *New Phytol.* **2018**, *218*, 167–182. [[CrossRef](#)]
75. Masutani, B.; Arimura, S.; Morishita, S. Investigating the mitochondrial genomic landscape of *Arabidopsis thaliana* by long-read sequencing. *PLoS Comput. Biol.* **2021**, *17*, e1008597. [[CrossRef](#)]
76. Vercellino, I.; Sazanov, L.A. The assembly, regulation and function of the mitochondrial respiratory chain. *Nat. Rev. Mol. Cell Biol.* **2022**, *23*, 141–161. [[CrossRef](#)]

**Disclaimer/Publisher's Note:** The statements, opinions and data contained in all publications are solely those of the individual author(s) and contributor(s) and not of MDPI and/or the editor(s). MDPI and/or the editor(s) disclaim responsibility for any injury to people or property resulting from any ideas, methods, instructions or products referred to in the content.